Trivalent Lanthanide Chalcogenolates: $Ln(SePh)_3$, $Ln_2(EPh)_6$, $Ln_4(SPh)_{12}$, and $[Ln(EPh)_3]_n$ (E = S, Se). How Metal, Chalcogen, and Solvent Influence Structure

Jongseong Lee, Deborah Freedman, Jonathan H. Melman, Meggan Brewer, Lei Sun, T. J. Emge, F. H. Long, and John G. Brennan*

Department of Chemistry, Rutgers, the State University of New Jersey, 610 Taylor Road, Piscataway, New Jersey 08854-8087

Received December 29, 1997

A series of trivalent lanthanide (Ln) benzenechalcogenolate (EPh, E = S, Se) complexes have been prepared and structurally characterized in an attempt to evaluate how metal size, chalcogen, and solvent influence structure and physical properties. The compounds $[(py)_3Ln(SPh)_3]_2$ (Ln = Ho (**1**) and Tm (**2**)), $[(py)_2Sm(SPh)_3]_4$ (**3**), $[(THF)Sm(SPh)_3]_{4n}$ (**4**), $(THF)_3Ln(SePh)_3$ (Ln = Tm (**5**), Ho (**6**), Er (**7**)), $[(py)_3Sm(SePh)_3]_2$ (**8**), and $[(THF)_4Ln_3(SePh)_9]_n$ (Ln = Pr (**9**), Nd (**10**), and Sm (**11**)) were isolated and characterized by IR, NMR, and UV−visible spectroscopy. Compounds **2**−**4**, **7**, **8**, and **10** have also been characterized by low-temperature single-crystal X-ray diffraction. Three trends in structure are clear. First, the tendency to form oligomeric structures is found to increase with the size of the lanthanide ion. Second, thiolates bridge metal ions to form polynuclear structures more effectively than selenolates. Finally, pyridine displaces bridging chalcogenolates to form less extended structures more effectively than THF. Compounds **5**−**7** are molecular *fac*-octahedral complexes, compounds **1**, **2**, and **8** are bimetallic molecules with a pair of chalcogen atoms spanning the pentagonal bipyramidal metal centers, compound **3** is a tetrametallic structure with an alternating (3-2-3) number of μ_2-thiolates spanning the linear assembly of four seven-coordinate Sm(III) ions, and compounds **4**, **9**, **10**, and **11** are polymers with sets of three doubly bridging benzenechalcogenolates connecting adjacent metal ions. Resonance Raman spectroscopy indicates that the intense electronic absorption associated with Sm(III) chalcogenolate is a chalcogen-to-metal charge-transfer excitation. Compounds **1** and **2** decompose thermally to give Ln_2S_3.

Introduction

The synthesis and characterization of lanthanide complexes in which chalcogenolates are the only anionic ligands $[Ln(ER)_x$: Ln = La−Yb; E = S, Se, Te; R = Ph,[1] substituted Ph,[2] SiR'_3,[3] 2-NC_5H_4,[4] CR'_3;[5] x = 2, 3) are motivated by fundamental questions related to the nature of the lanthanide−chalcogen bond and by the potential applications of these compounds for the synthesis of doped semiconductor,[6] fiber optic,[7] and pigment materials.[8]

The extent to which covalency contributes to the stability of Ln−E bonds remains an unanswered question. Lanthanide coordination chemistry has always been discussed in terms of ionic bonding, but there are compounds that have been described in more covalent terms.[9] While the Ln valence 4f shell is effectively shielded, these metals do have vacant 5d, 6s, and 6p orbitals that could overlap with ligand-based orbitals.[10] The

(1) (a) Berardini, M.; Emge, T.; Brennan, J. G. *J. Chem. Soc., Chem. Commun.* **1993**, 1537. (b) Berardini, M.; Emge, T.; Brennan, J. G. *J. Am. Chem. Soc.* **1993**, *115*, 8501. (c) Khasnis, D. V.; Lee, J.; Brewer, M.; Emge, T. J.; Brennan, J. G. *J. Am. Chem. Soc.* **1994**, *116*, 7129. (d) Brewer, M.; Khasnis, D.; Buretea, M.; Berardini, M.; Emge, T. J.; Brennan, J. G. *Inorg. Chem.* **1994**, *33*, 2743. (e) Berardini, M.; Emge, T. J.; Brennan, J. G. *J. Am. Chem. Soc.* **1994**, *116*, 6941. (f) Brewer, M.; Lee, J.; Brennan, J. G. *Inorg. Chem.* **1995**, *34*, 5919. (g) Lee, J.; Brewer, M.; Berardini, M.; Brennan, J. *Inorg. Chem.* **1995**, *34*, 3215. (h) Berardini, M.; Emge, T. J.; Brennan, J. G. *Inorg. Chem.* **1995**, *34*, 5327. (i) Geissinger, M.; Magull, J. *Z. Anorg. Allg. Chem.* **1995**, *621*, 2043. (j) Lee, J.; Emge, T. J.; Brennan, J. G. *Inorg. Chem.* **1997**, *36*, 5064.

(2) (a) Strzelecki, A. R.; Timinski, P. A.; Helsel, B. A.; Bianconi, P. A. *J. Am. Chem. Soc.* **1992**, *114*, 3159. (b) Mashima, K.; Nakayama, Y.; Kanehisa, N.; Kai, Y.; Nakamura, A. *J. Chem. Soc., Chem. Commun.* **1993**, 1847. (c) Strzelecki, A. R.; Likar, C. L.; Helsel, B. A.; Utz, T.; Lin, M. C.; Bianconi, P. A. *Inorg. Chem.* **1994**, *33*, 5188. (d) Mashima, K.; Nakayama, Y.; Fukumoto, H.; Kanehisa, N.; Kai, Y.; Nakamura, A. *J. Chem. Soc., Chem. Commun.* **1994**, 2523. (e) Tatsumi, K.; Amemiya, T.; Kawaguchi, H.; Tani, K. *J. Chem. Soc., Chem. Commun.* **1993**, 773. (f) Mashima, K.; Nakayama, Y.; Shibahara, T.; Fukumoto, H.; Nakamura, A. *Inorg. Chem.* **1996**, *35*, 93. (g) Froehlich, N.; Hitchcock, P. B.; Hu, J.; Lappert, M. F.; Dilworth, J. R. *J. Chem. Soc., Dalton Trans.* **1996**, 1941.

(3) (a) Cary, D.; Ball, G. E.; Arnold, J. *J. Am. Chem. Soc.* **1995**, *117*, 3492. (b) Cary, D. R.; Arnold, J. *Inorg. Chem.* **1994**, *33*, 1791. (c) Cary, D. R.; Arnold, J. *J. Am. Chem. Soc.* **1993**, *115*, 5, 2520.

(4) (a) Berardini, M.; Brennan, J. G. *Inorg. Chem.* **1995**, *34*, 6179. (b) Mashima, K.; Shibahara, T.; Nakayama, Y.; Nakamura, A. *J. Organomet. Chem.* **1995**, *501*, 263. (c) Berardini, M.; Lee, J.; Freedman, D.; Lee, J.; Emge, T. J.; Brennan, J. G. *Inorg. Chem.* **1997**, *36*, 5772.

(5) (a) Cetinkaya, B.; Hitchcock, P. B.; Lappert, M. F.; Smith, R. G. *J. Chem. Soc., Chem. Commun.* **1992**, 932. (b) Tatsumi, K.; Amemiya, T.; Kawaguchi, H.; Tani, K. *J. Chem. Soc., Chem. Commun*, **1993**, 773.

(6) (a) Pomrenke, G. S.; Klein, P. B.; Langer, D. W. *Rare Earth Doped Semiconductors*; MRS Symposium V. 301; Materials Research Society: Pittsburgh, PA, 1993. (b) Swiatek, K.; Godlewski, M.; Niinisto, L.; Leskela, M. *J. Appl. Phys.* **1993**, *74*, 3442. (c) Charreire, Y.; Marbeuf, A.; Tourillon, G.; Leskela, M.; Niinisto, L.; Nykanen, E.; Soininen, P.; Tolonen, O. *J. Electrochem. Soc.* **1992**, *139*, 619. (d) Harkonen, G.; Leppanen, M.; Soininen, E.; Tornquist, R.; Viljanen, J. *J. Alloys Compd.* **1995**, *225*, 552. (e) Charreire, Y.; Svoronos, D. R.; Ascone, I.; Tolonen, O.; Niinisto, L.; Leskela, M. *J. Electrochem. Soc.* **1993**, *140*, 2015. (f) Blasse, G. *J. Alloys Compd.* **1995**, *225*, 529. (g) Karpinska, K.; Godlewski, M.; Leskela, M.; Niinisto, L. *J. Alloys Compd.* **1995**, *225*, 544. (h) Ronda, C. R. *J. Alloys Compd.* **1995**, *225*, 534. (i) Pham-Thi, M. *J. Alloys Compd.* **1995**, *225*, 547. (j) Gorelenok, A. T.; Kamanin, A. V.; Shmidt, N. M. *Microelect. J.* **1995**, *26*, 705. (k) Guivarc'h, A.; Le Corre, A.; Sebilleau, D. *J. Mater. Res.* **1995**, *10*, 1942.

S0020-1669(97)01616-9 CCC: $15.00
Published on Web 05/02/1998

physical and chemical properties of $Ln(EPh)_3$ compounds are also crucial reference points for interpreting the bonding and physical properties of lanthanide chalcogenido clusters.[3a,11,12]

From an applied perspective, these chalcogenolate complexes are uniquely suited for delivering Ln ions into chalcogenido materials[6,7] because ER ligands are excellent leaving groups. Such reactivity was noted recently in the synthesis of the $[Sm_7S_7(SePh)_6(DME)_7]^+$ and $Gd_8S_6(SPh)_{12}(THF)_8$ from the reactions of $Ln(EPh)_3$ with elemental S.[11] The facility with which ER ligands are displaced at room temperature suggests that $Ln(ER)_3$ will find numerous synthetic applications. Importantly, the thiolate study[11b] illustrated that the redox inactive Ln ions are potentially as reactive as the redox active ($Ln^{2+/3+}$) Sm, Eu, and Yb. Such reactivity provides additional impetus for investigating the synthetic chemistry and the physical properties of all $Ln(ER)_3$, particularly given the unusual structural/reactivity trends noted in lanthanide chloride chemistry.[13]

This manuscript extends our initial efforts in $Ln(EPh)_3$ chemistry to the middle of the lanthanide series. The synthesis and characterization of $[(py)_3Ln(SPh)_3]_2$ (Ln = Ho (**1**) and Tm (**2**)), $[(py)_2Sm(SPh)_3]_4$ (**3**), $[(THF)Sm(SPh)_3]_{4n}$ (**4**), $(THF)_3Ln(SePh)_3$ (Ln = Tm (**5**), Ho (**6**), Er (**7**)), $[(py)_3Sm(SePh)_3]_2$ (**8**), and $[(THF)_4Ln_3(SePh)_9]_n$ (Ln = Pr (**9**), Nd (**10**), and Sm (**11**)) are described. The effect of metal size, chalcogenolate, and neutral donors on solid-state structure is assessed, and the assignment of the electronic spectra of the redox active $Ln(ER)_3$ compounds to a LMCT excitation is confirmed by resonance Raman spectroscopy.

Experimental Section

General Methods. All syntheses were carried out under ultrapure nitrogen (JWS), using conventional drybox or Schlenk techniques. Solvents (Fisher) were refluxed continuously over molten alkali metals or sodium/benzophenone and collected immediately prior to use. Anhydrous pyridine (Aldrich) was purchased and refluxed over KOH. PhSeSePh and PhSSPh were purchased from either Aldrich or Strem and recrystallized from hexane. Ln and Hg were purchased from Strem. Melting points were taken in sealed capillaries and are uncorrected. IR spectra were taken on a Mattus Cygnus 100 FTIR spectrometer and recorded from 4000 to 450 cm^{-1} as a Nujol mull on KBR plates. Electronic spectra were recorded on a Varian DMS 100S spectrometer with the samples in a 0.10 mm quartz cell attached to a Teflon stopcock. Elemental analyses were performed by Quantitative Technologies, Inc. (Salem, NJ). These compounds are sensitive to the thermal dissociation of neutral donor ligands at room temperature and so the experimentally determined elemental analyses are generally found to be lower than the computed analyses. Products appear homogeneous, and for every sample several crystals of each compound were examined by single-crystal X-ray diffraction in an attempt to find a crystal suitable for a complete structural determination. The same unit cell was obtained consistently for each compound. Twinning and a likely phase transition were found to be problematic in a number of samples. NMR spectra were obtained on either a Varian Gemini 200 MHz or Varian 400 MHz NMR spectrometer at 23 °C and are reported in δ (ppm). Powder diffraction spectra were obtained from a Scintag Pad V diffractometer and Cu Kα radiation. Raman spectra were recorded using a Coherent Innova 90 Ar/Kr mixed gas laser, a Spex model 1877E triple monochromator, and a Spex spectrum one charge-coupled-detector cooled with liquid nitrogen. Blue (488 nm), green (514 nm), and yellow (567 nm) light were used. The average power irradiating the sample was 100 mW. A laser prefilter Spex model 1450 was used to reject plasma lines from the laser tube. The samples were held at room temperature in a cuvette sealed with a Teflon stopcock and aligned such that the collection of scattered light was in a backscattered geometry. The polarization of the laser light, both incident and collected, was unspecified. Calibration of the Raman spectra was carried out using known atomic emission lamps and is accurate to approximately 1 cm^{-1}.

Synthesis of $[(pyridine)_3Ho(SPh)_3]_2$ (1). Ho (0.66 g, 4.0 mmol), Ph_2S_2 (1.31 g, 6 mmol), and Hg (55 mg, 0.27 mmol) were added to pyridine (40 mL), and the mixture was stirred for 3 days as the solution color turned peach. The solution was filtered, concentrated to 20 mL, and layered with diethyl ether (60 mL). After 1 day, peach colored crystals (2.10 g, 72%; mp 127 °C) were collected. Anal. Calcd for $C_{33}H_{30}N_3HoS_3$: C, 54.0; H, 4.12; N, 5.72. Found: C, 50.1; H, 3.86; N, 5.47. IR: 2922 (b), 2743 (s), 2669 (s), 1949 (s), 1862 (s), 1633 (s), 1577 (m), 1477 (m), 1376 (m), 1303 (s), 1261 (m), 1218 (m), 1147 (m), 1082 (s), 1026 (m) 894 (s), 803 (s), 734 (m), 700 (m), 602 (s), 480 (m), 412 (m) cm^{-1}. No ^1H NMR (20 mgs in 0.50 mL of $CD_3S(O)CD_3$) resonances were detected. The compound does not show a λ_{max} from 350 to 800 nm in either THF or pyridine. Unit cell (Mo Kα radiation, −120 °C): $a = 24.154(6)$ Å, $b = 14.214(5)$ Å, $c = 20.580(8)$ Å, $\beta = 96.43(2)°$, $V = 7021(4)$ Å^3. Thermolysis: **1** (650 mg) was placed in a Pyrex tube under vacuum for 1 h. The tube was then sealed, and the sample temperature was raised over a period of 3 days from 50 to 300 °C, with one end of the tube kept at room temperature. Between 80 and 100 °C, a colorless liquid (pyridine) condensed in the part of the tube that was outside the furnace. Between 250 and 300 °C, yellow diphenyl sulfide condensed in the cold part of the sample holder. The volatile materials were identified by ^1H NMR spectroscopy. The remaining black solid (220 mg, 100.6%) was transferred to a quartz tube that was then sealed under vacuum (10^{-7} Torr). Further heating (1000 °C, 3 days) showed no further elimination of volatile products, and an X-ray powder diffraction spectrum of the final solid product revealed the presence of microcrystalline Ho_2S_3.[14] Similarly, thermolysis of **2** gave Tm_2S_3.[15]

Synthesis of $[(pyridine)_3Tm(SPh)_3]_2$ (2). Tm (0.68 g, 4.0 mmol), Ph_2S_2 (1.31 g, 6 mmol), and Hg (55 mg, 0.27 mmol) were added to pyridine (40 mL), and the mixture was stirred for 3 days as the solution color turned yellow green. The solution was filtered, concentrated to 20 mL, and layered with diethyl ether (60 mL). After 1 day, yellow green crystals (2.42 g, 82.3%; mp 110 °C) were collected. Anal. Calcd

(7) (a) Wang, J.; Hector, J. R.; Payne, D. N. *Appl. Phys. Lett*. **1997**, *71*, 1753. (b) Jurdyc, A. M.; Garapon, C.; Adam, J. L. *J. Non-Cryst. Solids* **1997**, *213/4*, 231. (c) Quimby, R. S.; Aitken, B. G. *J. Appl. Phy*. **1997**, *82*, 3992. (d) Schweizer, T.; Hewak, D. W.; Payne, D. N. *Opt. Lett.* **1996**, *21*, 1594. (e) Kumta, P. K.; Risbud, S. H. *J. Mater. Sci.* **1994**, *29*, 1135. (f) Kumta, P. K.; Risbud, S. H, *Prog. Cryst. Growth Char.* **1991**, *22*, 321. (g) Nishii, J.; Morimoto, S.; Yokota, R.; Yamagishi, T. *J. Non-Cryst. Solids* **1987**, *95/6*, 641. (h) Savage, J. A. In *Infrared Optical Materials and Their Antireflection Coatings*; Adam Hilger Ltd.: Bristol, U.K., 1985; pp 79−94. (i) Nishii, J.; Morimoto, S.; Inagawa, I.; Iizuka, R.; Yamashita, T.; Yokota, R.; Yamagishi, T *J. Non-Cryst. Solids* **1982**, *140*, 199. (j) Sanghara, J. S.; Busse, L. E.; Aggarwall, I. D. *J. Appl. Phys.* **1994**, *75*, 4885. (k) Katsugama, T.; Matsumura, H. *J. Appl. Phys.* **1994**, *75*, 2743.

(8) (a) Chopin, T.; Guichon, H.; Touret, O. U.S. Patent No. 5, 348, 581, 1994. (b) Chopin; T.; Dupuis; D. U.S. Patent No. 5, 401, 309, 1995.

(9) (a) King, W. A.; Di Bella, S.; Marks, T. J. *J. Am. Chem. Soc*. **1996**, *118*, 627. (b) King, W. A.; Marks, T. J.; Anderson, D. M. *J. Am. Chem. Soc.* **1992**, *114*, 9221. (c) Brennan, J.; Cloke, F. G. N.; Sameh, A.; Zalkin, A. *J. Chem. Soc. Chem. Commun*. **1987**, 1668. (d) Anderson, D.; Cloke, F. G. N.; Cox, P.; Edelstein, N.; Green, J.; Pang, T.; Sameh, A.; Shalimoff, G. *J. Chem. Soc., Chem. Commun.* **1989**, 53. (e) Anderson, D.; Cloke, F. G. N.; Cox, P. *J. Chem. Soc., Chem. Commun*. **1990**, 284.

(10) (a) Gerth, G.; Kienle, P.; Luchner, K. *Phys. Lett. A* **1968**, *27*, 557. (b) Eatough, N. L.; Hall, H. T. *Inorg. Chem.* **1970**, *9*, 417. (c) Dagys, R. S.; Anisimov, F. G. *Sov. Phys. Solid State* **1984**, *26*, 547. (d) Wachter, P. *Crit. Rev. Solid State* **1972**, *3*, 189. (e) Byrom, E.; Ellis, D. E.; Freeman, A. J. *Phys. Rev. B* **1976**, *14*, 3558. (f) Zhukov, V. P.; Gubanov, V. A.; Weber, J. *J. Chem. Phys. Solids* **1981**, *42*, 631.

(11) (a) Freedman, D.; Emge, T. J.; Brennan, J. G. *J. Am. Chem. Soc.* **1997**, *119*, 11112. (b) Melman, J. H.; Emge, T. J.; Brennan, J. G. *Chem. Commun.* **1997**, 2269.

(12) (a) Evans, W. J.; Rabe, G.; Ziller, J. *Angew. Chem., Int. Ed. Engl.* **1994**, *33*, 2110. (b) Pernin, C. G.; Ibers, J. A. *Inorg. Chem*. **1997**, *36*, 3802.

(13) Evans, W. J.; Shreeve, J. L.; Doedens, R. J. *Inorg. Chem*. **1995**, *34*, 576.

(14) JCPDS File 44-1156.

(15) JCPDS File 44-1157.

for $C_{33}H_{30}N_3TmS_3$: C, 54.0; H, 4.12; N, 5.72. Found: C, 48.9; H, 3.45; N, 5.54. IR: 2922 (b), 2854 (m), 1950 (m), 1861 (s), 1634 (s), 1577 (m), 1459 (m), 1377 (s), 1261 (s), 1218 (s), 1146 (s), 1067 (s), 1027 (s), 896 (m), 805 (m), 737 (m), 699 (m), 603 (m), 484 (m), 412 (m) cm^{-1}. ^1H NMR (20 mg in 0.50 mL NC_5D_5) contained resonances at 8.11, 7.51, and 7.15 ppm which were too broad for accurate integration. The compound does not show a λ_{max} from 350 to 800 nm in either THF or pyridine.

Synthesis of [(pyridine)$_2$Sm(SPh)$_3$]$_4$ (3). Sm (0.35 g, 2.4 mmol), Ph_2S_2 (0.81 g, 3.7 mmol), and Hg (0.05 g, 0.24 mmol) were added to pyridine (40 mL). After being stirred for 3 days, the resultant yellow-green solution was filtered, concentrated to ca. 20 mL, and layered with ether to give light yellow crystals (0.73 g, 46%; the compound does not melt but appears to lose solvent at ca. 120 °C and decompose at 385 °C). The compound crystallizes with one lattice diethyl ether/Sm_4 molecule. Anal. Calcd for $C_{116}H_{110}ON_8Sm_4S_{12}$: C, 53.2; H, 4.23; N, 4.28. Found: C, 45.0; H, 3.76; N, 2.49. IR: 2920 (br), 1598 (w), 1576 (w), 1461 (s), 1377 (s), 1260 (w), 1217 (w), 1083 (w), 1062 (w), 1023 (w), 1004 (w), 739 (m), 700 (s), 623 (w), 601 (w) cm^{-1}. ^1H NMR (ca. 25 mg in 0.60 mL CD_3CN) showed only resonances due to displaced pyridine. The compound does not show a λ_{max} from 350 to 800 nm in pyridine.

Synthesis of [(THF)Sm(SPh)$_3$]$_{4n}$ (4). Sm (0.453 g, 3.01 mmol), Ph_2S_2 (0.986 g, 4.52 mmol), and Hg (35 mg, 0.18 mmol) were combined in THF (40 mL). The mixture was stirred for 24 h until metal was consumed, and then the cloudy green solution was filtered. The resultant yellow solution was layered with hexane to give yellow crystals (0.363 g, 22%; the crystals do not melt but darken at 97 °C and then progressively lose color from 280 to 300 °C). IR: 1574 (w), 1081 (w), 858 (w), 732 (m), 689 (m), 481 (w) cm^{-1}. ^1H NMR (OC_4D_8) shows only broad peaks due to displaced THF at 3.58 and 1.73 ppm. Anal. Calcd for $C_{22}H_{23}OS_3Sm$: C, 48.05; H, 4.21. Found: C, 43.40; H, 4.13. The compound does not show a λ_{max} from 350 to 800 nm in THF.

Synthesis of (THF)$_3$Tm(SePh)$_3$ (5). Tm (0.68 g, 4.0 mmol), Ph_2Se_2 (1.87 g, 6.0 mmol), and Hg (55 mg, 0.27 mmol) were added to THF (40 mL), and the mixture was stirred for 3 days as the solution color turned yellow-green. The solution was filtered, concentrated to 20 mL, and layered with hexane (60 mL). After 1 day crystals (1.80 g, 53%; desolvates at 110 °C and decomposes at 310 °C) were collected. Anal. Calcd for $C_{30}H_{39}O_3TmSe_3$: C, 42.2; H, 4.61. Found: C, 36.7, 38.37; H, 4.68, 3.03. IR: 2969 (b), 2748 (s), 2592 (s), 2532 (s), 2317 (s), 2317 (s), 2241 (s), 2068 (s), 1943 (m), 1865 (m), 1804 (m), 1737 (m), 1637 (m), 1567 (m), 1448 (m), 1384 (m), 1296 (m), 1263 (m), 1177 (m), 966 (b), 732 (m), 701 (m), 511 (m), 480 (m), 422 (m) cm^{-1}. ^1H NMR (20 mg in 0.50 mL of $CD_3S(O)CD_3$) contained resonances at 7.24, 6.65 (phenyl group) and 3.68, 1.83 (THF) ppm which were too broad for accurate integration. The compound does not show a λ_{max} from 350 to 800 nm in either THF or pyridine.

Synthesis of (THF)$_3$Ho(SePh)$_3$ (6). Ho (0.66 g, 4.0 mmol), Ph_2Se_2 (1.87 g, 5.99 mmol), and Hg (55 mg, 0.27 mmol) were added to THF (40 mL), and the mixture was stirred for 3 days as the solution color turned pink. The solution was filtered, concentrated to 20 mL, and layered with hexane (60 mL). After 1 day, colorless crystals (2.62 g, 77.2%; mp 120 °C (desolvates), 330 °C (dec)) were collected. Anal. Calcd for $C_{30}H_{39}O_3HoSe_3$: C, 42.42; H, 4.63. Found: C, 38.16; H, 4.27. IR: 2922 (w), 2727 (s), 2677 (s), 2357 (s), 1572 (m), 1462 (m), 1377 (m), 1294 (s), 1260 (m), 1073 (m), 1080 (m), 913 (s), 855 (s), 803 (m), 731 (m), 693 (m), 664 (m), 468 (m). No ^1H NMR (20 mg in 0.50 mL of $CD_3S(O)CD_3$) resonances were detected. The compound does not show a λ_{max} from 350 to 800 nm in either THF or pyridine.

Synthesis of (THF)$_3$Er(SePh)$_3$ (7). Er (0.54 g, 3.2 mmol), Hg (100 mg, 0.49 mmol), and Ph_2Se_2 (1.5 g, 4.8 mmol) were stirred in THF (45 mL) for 24 h. The pale pink solution was filtered, concentrated to ca. 30 mL, and allowed to sit at −20 °C for 1 day, after which $(THF)_3Er(SePh)_3$ (2.3 g, 72%; mp 225 °C (dec)) was isolated as pale pink needles. Anal. Calcd for $C_{30}H_{39}O_3ErSe_3$: C, 42.3; H, 4.62. Found: C, 40.9; H, 4.70. IR: 2968 (b), 1865 (s), 1806 (s), 1734 (s), 1572 (m), 1468 (m), 1385 (s), 1330 (s), 1295 (s), 1248 (s), 1178 (s), 1036 (s), 902 (s), 859 (s), 733 (m), 695 (m), 667 (m), 468 (s) cm^{-1}. ^1H NMR (20 mg in 0.50 mL of $CD_3S(O)CD_3$) contained resonances at 7.17 (2 H), 6.58 (3 H) and 3.60 (4 H), 1.75 (4 H) ppm. The compound does not show a λ_{max} from 350 to 800 nm in either THF or pyridine.

Synthesis of [(pyridine)$_3$Sm(SePh)$_3$]$_2$ (8). Sm (0.61 g, 4.0 mmol), Ph_2Se_2 (1.87 g, 5.99 mmol), and Hg (55 mg, 0.27 mmol) were added to pyridine (40 mL), and the mixture was stirred for 3 days as the solution color turned red. The solution was filtered, concentrated to 20 mL, and layered with diethyl ether (60 mL). After 1 day, peach crystals (2.10 g, 61.4%; it started to lose its solvents very slowly from 135 °C and decomposed at 300 °C) were collected. Anal. Calcd for $C_{33}H_{30}N_3Se_3Sm$: C, 46.3; H, 3.53; N, 4.90. Found: C, 43.28; H, 3.59; N, 4.48. IR: 2935 (w), 2723 (s), 2668 (s), 2466 (s), 2372 (s), 2019 (s), 2310 (s) 1935 (s), 1861 (s), 1796 (s), 1735 (s), 1686 (s), 1629 (s), 1595 (m), 1456 (m), 1375 (m), 1300 (s), 1261 (s), 1216 (m), 1152 (m), 1067 (m), 1001 (m), 936 (s), 893 (s), 836 (s), 799 (s), 731 (m), 700 (s), 622 (s), 602 (s), 465 (m), 404 (m) cm^{-1}. ^1H NMR (40 mg in 0.50 mL of NC_5D_5) contained resonances at 8.70 (2 H), 7.79 (1 H), 7.55 (2 H), 7.21 (3 H), and 6.96 (2 H) ppm. The visible spectrum is concentration dependent. UV: λ_{max} (ca. 1 mg/mL of pyridine) = 425 nm.

Synthesis of [(THF)$_4$Pr$_3$(SePh)$_9$]$_n$ (9). Pr (286 mg, 2.0 mmol), Ph_2Se_2 (938 mg, 3.0 mmol), and Hg (50 mg, 0.25 mmol) were stirred in THF (50 mL) for 3 days. The yellow solution was filtered, concentrated to 30 mL, and layered with hexanes (30 mL) to give pale green needles (0.40 g, 27%; the compounds does not melt but turns orange at ca. 200 °C and continues to darken up to 300 °C). Anal. Calcd for $C_{70}H_{77}O_4Pr_3Se_9$: C, 39.8; H, 3.76. Found: C, 38.1; H, 3.82. IR: 3173 (w), 2932 (s), 2726 (w), 2343 (w), 1571 (m), 1461 (s), 1377 (s), 1306 (w), 1263 (w), 1169 (w), 1154 (w), 1067 (m) 1021 (m), 974 (w), 854 (m), 752 (s), 688 (m), 668 (w), 615 (w), 462 (w), 451 (w) cm^{-1} . ^1H NMR (NC_5D_5, 25 °C) spectrum contained broad phenyl resonances at 6.37 (2H) and 5.26 (3H) ppm and resonances from displaced THF at 3.58 and 1.73 ppm. The compound does not show a λ_{max} from 350 to 800 nm in either THF or pyridine. Unit cell (Mo Kα radiation, −120 °C): a = 34.793(21) Å, b = 25.791(9) Å, c = 26.882(11) Å, β = 130.78(4)°, V = 18267(18) Å^3.

Synthesis of [(THF)$_4$Nd$_3$(SePh)$_9$]$_n$ (10). Nd (0.58 g, 4.0 mmol), Ph_2Se_2 (1.89 g, 6.0 mmol), and Hg (50 mg, 0.25 mmol) were stirred in THF (50 mL) for 2 days. The light blue solution was filtered, concentrated (40 mL), and layered with hexanes (30 mL). Colorless crystals formed after 1 day (2.6 g, 89%). X-ray-quality crystals were obtained by recrystallization and layering with pentane (20 mL). The crystals did not melt but turned gray at ca. 140 °C, light brown by 230 °C, and continued to darken up to 300 °C. Anal. Calcd for $C_{70}H_{77}O_4Nd_3Se_9$: C, 39.5; H, 3.65. Found: C, 37.8; H, 3.66. IR: 3167 (w), 2911 (s), 2725 (w), 2674 (w), 2364 (w), 1571 (m), 1461 (s), 1378 (s), 1304 (w), 1208 (w), 1169 (w), 1155 (w), 1071 (m), 1019 (m), 974 (w), 915 (w), 855 (m), 826 (w), 728 (s), 689 (s), 664 (m), 614 (w), 464 (s) cm^{-1}. ^1H NMR (NC_5D_5N, 25 °C): phenyl protons, 6.86 (2H, b), 5.59 (2H, b), and 5.27 (1H, b) and displaced THF at 3.58 and 1.73 ppm. The compound does not show a λ_{max} from 350 to 800 nm in either THF or pyridine.

Synthesis of [(THF)$_4$Sm$_3$(SePh)$_9$]$_n$ (11). Sm (0.61 g, 4.0 mmol), Ph_2Se_2 (1.87 g, 5.99 mmol), and Hg (55 mg, 0.27 mmol) were added to THF (40 mL), and the mixture was stirred for 3 days as the solution color turned red. The solution was filtered, concentrated to 20 mL, and layered with hexane (60 mL). After 1 day, red crystals (2.20 g, 79.7%; the compound desolvates at 135 °C and appears to decompose at 300 °C) were collected. Anal. Calcd for $C_{70}H_{77}O_4Se_9Sm_3$: C, 39.3; H, 3.63. Found: C, 37.7; H, 2.85. IR: 2927 (w), 2725 (s), 2680 (s), 1946 (s), 1875 (s), 1810 (s), 1713 (s), 1571 (m), 1451 (m), 1376 (m), 1297 (s), 1260 (s), 1171 (s), 1067 (m), 1018 (m), 912 (s), 842 (m), 824 (m), 802 (s), 728 (m), 664 (m), 689 (m), 464 (m) cm^{-1}. ^1H NMR (20 mg in 0.50 mL of $CD_3S(O)CD_3$) contained resonances at 7.34 (18 H), 6.58 (27 H) and 3.57 (16 H), 1.72 (16 H) ppm. UV: λ_{max} (ca. 1 mg/mL of THF) = 409 nm. Unit cell (Mo Kα radiation, −120 °C): a = 34.109(15) Å, b = 25.342(8) Å, c = 26.877(13) Å, β = 129.08(3)°, V = 18034(16) Å^3.

X-ray Structure Determination of 2−4, 7, 8, and 10. Data for **2**−**4**, **7**, **8**, and **10** were collected on an Enraf-Nonius CAD4 diffractometer with graphite-monochromatized Mo Kα radiation (λ = 0.710 73 Å) at low temperature. The check reflections measured every 1 h

Table 1. Summary of Crystallographic Details for $[(py)_3Tm(SPh)_3]_2$ (**2**), $[(py)_2Sm(SPh)_3]_4$ (**3**), $[(THF)Sm(SPh)_3]_{4n}$ (**4**), $(THF)_3Er(SePh)_3$ (**7**), $[(py)_3Sm(SePh)_3]_2$ (**8**), and $[(THF)_4Nd_3(SePh)_9]_n$ (**10**)

	compound					
	2	**3**	**4**	**7**	**8**	**10**
empirical formula	$C_{38}H_{35}N_4S_3Tm$	$C_{60}H_{60}N_4OS_6Sm_2$	$C_{88}H_{92}O_4S_{12}Sm_4$	$C_{30}H_{39}ErO_3Se_3$	$C_{35.5}H_{32.5}N_{3.5}Se_3Sm$	$C_{72}H_{81}Nd_3O_{4.5}Se_9$
fw	812.81	1346.18	2199.74	851.75	895.38	8646.91
space group	*C*2/*c*	$P2_1/n$	*C*2/*c*	*P*31*c*	$P\bar{1}$	*C*2/*c*
a (Å)	24.105(6)	13.488(2)	27.780(7)	15.272(3)	10.494(6)	34.232(9)
b (Å)	14.228(2)	31.085(7)	14.177(6)	15.272(3)	12.863(4)	25.526(11)
c (Å)	20.576(2)	14.429(2)	44.949(13)	7.887(1)	14.584(4)	27.358(12)
α (deg)	90	90	90	90	69.55(2)	90
β (deg)	96.50(2)	102.37(2)	95.61(2)	90	80.12(3)	128.93(2)
γ (deg)	90	90	90	120	68.47(3)	90
V (Å^3)	7011(3)	5909(2)	17618(10)	1593.1(6)	1714(1)	18596(12)
Z	8	4	8	2	2	8
D_{calc} (g/cm^3)	1.540	1.513	1.659	1.776	1.735	1.544
temp (°C)	−120	−120	−120	−120	−120	−70
λ (Å)	0.710 73	0.710 73	0.710 73	0.710 73	0.710 73	0.710 73
abs coeff (mm^{-1})	2.74	2.22	2.96	6.09	4.93	5.210
$R(F)$ $[I > 2\sigma(I)]$[a]	0.025	0.052	0.033	0.018	0.039	0.077
$R_w(F^2)$ $[I > 2\sigma(I)]$[a]	0.061	0.111	0.061	0.041	0.104	0.186

[a] Definitions: $R(F_o) = \sum||F_o| - |F_c||/\sum|F_o|$ and $R_w(F^2) = \{\sum[w(F_o^2 - F_c^2)^2]/\sum[w(F_o^2)]^2\}^{1/2}$. Additional crystallographic details are given in the Supporting Information.

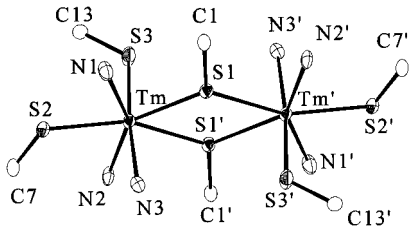

Figure 1. Molecular structure of dimeric $[(py)_3Tm(SPh)_3]_2$ with most of the C and H atoms removed for clarity. Thermal ellipsoids for all structures are shown at the 50% probability level.

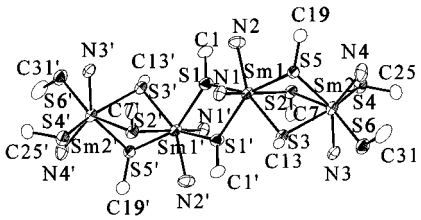

Figure 2. Molecular structure of tetrametallic $[(py)_2Sm(SPh)_3]_4$ with most of the C and H atoms removed for clarity.

showed less than 2% intensity variation for all samples except **10**, which showed an 8% decay. The data were corrected for Lorenz effects, polarization, and absorption, the latter by a numerical (SHELX76)[16] method. The structures were solved by Patterson methods (SHELXS-86).[17] All non-hydrogen atoms were refined (SHELXL93 or SHELXL97) based upon F_o^2. All hydrogen atom coordinates were calculated with idealized geometries (SHELXL93).[18] Scattering factors (f_o, f', f'') are as described in SHELXL93. Crystallographic data and final *R* indices for all compounds are given in Table 1. Significant bond distances and angles for **2**−**4**, **7**, **8**, and **10** are given in Tables 2−7, respectively. Complete crystallographic details are given in the Supporting Information. ORTEP diagrams[19] of **2**−**4**, **7**, **8**, and **10** are shown in Figures 1−6, respectively. Thermal ellipsoids are shown at the 50% probability level.

Results

Ln(SPh)$_3$. Lanthanide benzenethiolates are conveniently prepared in high yield by the direct reduction of disulfide with elemental Ln, and the presence of Hg increases the rate of product formation. The products are soluble in strong donor solvents such as pyridine, from which the bimetallic coordination

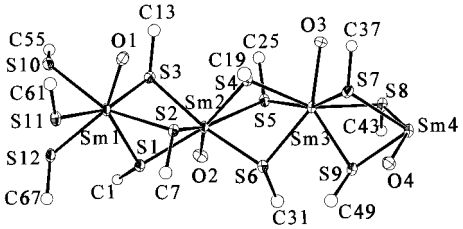

Figure 3. Molecular structure of the repeating unit in polymeric $[(THF)Sm(SPh)_3]_n$ with most of the C and H atoms removed for clarity.

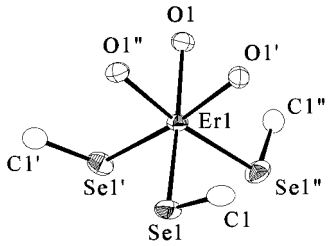

Figure 4. Molecular structure of octahedral $(THF)_3Er(SePh)_3$ with most of the C and H atoms removed for clarity.

complexes $[(py)_3Ln(SPh)_3]_2$ (Ln = Ho (**1**) and Tm (**2**)) can be isolated by fractional crystallization in 70−80% yield. Both **1** and **2** were characterized by conventional methods, and **2** was studied by low-temperature single-crystal X-ray diffraction (Figure 1, Table 2). The Ho derivative was found to be isostructural with **2**. Complex **2** is dimeric, with a pair of μ_2-thiolates bridging the seven coordinate Tm(III) ions. There are terminal benzenethiolate ligands in both the axial and equatorial positions of each of the inversion related pentagonal bipyramids. These nonredox active thiolates have the light colors that are characteristic of lanthanide ions. The products of the thermal

(16) Sheldrick, G. M. SHELX76, Program for Crystal Structure Determination, University of Cambridge, England, 1976.
(17) Sheldrick, G. M. SHELXS86, Program for the Solution of Crystal Structures, University of Göttingen, Germany, 1986.
(18) (a) Sheldrick, G. M. SHELXL93, Program for Crystal Structure Refinement, University of Göttingen, Germany, 1993. (b) Sheldrick, G. M. SHELXL97, Program for Crystal Structure Refinement, University of Göttingen, Germany, 1997.
(19) (a) Johnson, C. K. *ORTEP II*; Report ORNL-5138; Oak Ridge National Laboratory: Oak Ridge, TN, 1976. (b) Zsolnai, L. XPMA and ZORTEP, Programs for Interactive ORTEP Drawings, University of Heidelberg, Germany, 1997.

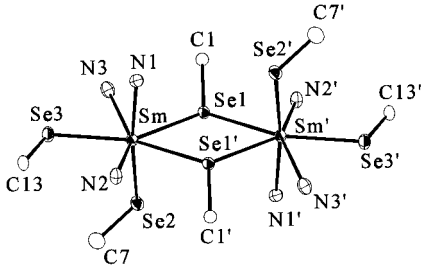

Figure 5. Molecular structure of dimeric $[(py)_3Sm(SePh)_3]_2$ with most of the C and H atoms removed for clarity.

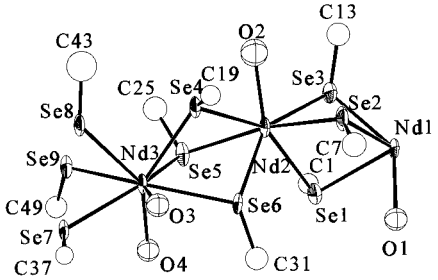

Figure 6. Molecular structure of the repeating unit in polymeric $[(THF)_4Nd_3(SePh)_9]_n$ with most of the C and H atoms removed for clarity.

Table 2. Significant Bond Lengths (Å) and Angles (deg) for $[(py)_3Tm(SPh)_3]_2$[a]

Tm−N(2)	2.448(3)	Tm−N(1)	2.453(3)
Tm−N(3)	2.506(3)	Tm−S(3)	2.6980(11)
Tm−S(2)	2.7126(10)	Tm−S(1)	2.7914(10)
Tm−S(1′)	2.8258(11)	S(1)−C(1)	1.769(3)
S(1)−Tm′	2.8257(11)	S(2)−C(7)	1.766(4)
S(3)−C(13)	1.766(3)		
N(2)−Tm−N(1)	147.14(9)	N(2)−Tm−N(3)	86.60(10)
N(1)−Tm−N(3)	93.04(10)	N(2)−Tm−S(3)	91.85(7)
N(1)−Tm−S(3)	91.54(8)	N(3)−Tm−S(3)	173.75(6)
N(2)−Tm−S(2)	79.08(7)	N(1)−Tm−S(2)	68.17(7)
N(3)−Tm−S(2)	85.15(7)	S(3)−Tm−S(2)	100.51(3)
N(2)−Tm−S(1)	137.13(6)	N(1)−Tm−S(1)	75.26(7)
N(3)−Tm−S(1)	84.21(7)	S(3)−Tm−S(1)	92.86(3)
S(2)−Tm−S(1)	141.19(3)	N(2)−Tm−S(1′)	75.80(7)
N(1)−Tm−S(1′)	137.06(7)	N(3)−Tm−S(1′)	89.56(7)
S(3)−Tm−S(1′)	84.19(3)	S(2)−Tm−S(1′)	154.59(2)
S(1)−Tm−S(1′)	62.37(3)	C(1)−S(1)−Tm	118.01(11)
C(1)−S(1)−Tm′	119.24(11)	Tm−S(1)−Tm′	117.63(3)
C(7)−S(2)−Tm	117.50(11)	C(13)−S(3)−Tm	122.95(12)

[a] Symmetry transformations used to generate equivalent atoms: (′) $-x + 1/2, -y + 3/2, -z$.

decomposition of **1** and **2** were identified as Ln_2S_3 by X-ray powder diffraction.

Toward the middle of the lanthanide series, complex solubility decreases, but a pyridine coordination complex of $Sm(SPh)_3$ can be isolated as light yellow crystals by fractional crystallization. A low-temperature diffraction study identified the structure as tetrametallic $[(pyridine)_2Sm(SPh)_3]_4$ (**3**), a nonlinear array of four Sm(III) ions having distorted seven coordinate pentagonal bipyramidal geometries (Figure 2, Table 3). The two exterior Sm(III) ions in **3** have terminal benzenethiolates in both axial and equatorial positions, and these ions are bridged to the two interior Sm ions by sets of three μ_2-SPh ligands. The two internal Sm ions are connected by a pair of μ_2-SPh ligands. The coordination sphere of each of the two inner Sm(III) ions are composed of five bridging PhS and two py ligands, while the inner sphere of each exterior Sm ion contains two pyridine, three bridging, and two terminal thiolates.

Table 3. Significant Bond Lengths (Å) and Angles (deg) for $[(py)_2Sm(SPh)_3]_4$[a]

Sm(1)−N(2)	2.517(9)	Sm(1)−N(1)	2.535(9)
Sm(1)−S(2)	2.785(3)	Sm(1)−S(1)	2.825(3)
Sm(1)−S(1′)	2.842(3)	Sm(1)−S(3)	2.844(3)
Sm(1)−S(5)	2.847(3)	Sm(2)−N(4)	2.581(10)
Sm(2)−N(3)	2.647(9)	Sm(2)−S(6)	2.752(3)
Sm(2)−S(4)	2.756(3)	Sm(2)−S(2)	2.891(3)
Sm(2)−S(3)	2.903(3)	Sm(2)−S(5)	2.906(3)
S(1)−C(1)	1.775(11)	S(1)−Sm(1)′	2.842(3)
S(2)−C(7)	1.775(11)	S(3)−C(13)	1.765(11)
S(4)−C(25)	1.758(11)	S(5)−C(19)	1.781(12)
S(6)−C(31)	1.804(14)		
C(1)−S(1)−Sm(1)	120.3(4)	C(1)−S(1)−Sm(1)′	120.6(4)
C(7)−S(2)−Sm(1)	122.2(4)	C(7)−S(2)−Sm(2)	111.7(4)
C(13)−S(3)−Sm(1)	115.7(3)	C(13)−S(3)−Sm(2)	117.9(4)
C(25)−S(4)−Sm(2)	114.0(5)	C(19)−S(5)−Sm(1)	118.4(4)
C(19)−S(5)−Sm(2)	117.2(4)	C(31)−S(6)−Sm(2)	117.6(4)

[a] Symmetry transformations used to generate equivalent atoms: (′) $-x + 1, -y + 1, -z$.

Table 4. Significant Bond Lengths (Å) and Angles (deg) for $[(THF)Sm(SPh)_3]_{4n}$[a]

Sm(1)−S(3)	2.842(2)	Sm(1)−S(11)	2.845(2)
Sm(1)−S(1)	2.854(2)	Sm(1)−S(10)	2.855(2)
Sm(1)−S(2)	2.878(2)	Sm(1)−S(12)	2.894(3)
Sm(1)−Sm(2)	4.0893(13)	Sm(2)−O(2)	2.414(6)
Sm(2)−S(6)	2.765(2)	Sm(2)−S(3)	2.823(2)
Sm(2)−S(1)	2.835(2)	Sm(2)−S(4)	2.876(3)
Sm(2)−S(2)	2.896(2)	Sm(2)−S(5)	2.945(2)
Sm(3)−O(3)	2.515(5)	Sm(3)−S(8)	2.815(2)
Sm(3)−S(4)	2.821(2)	Sm(3)−S(7)	2.820(3)
Sm(3)−S(5)	2.853(2)	Sm(3)−S(9)	2.869(2)
Sm(3)−S(6)	2.893(3)	Sm(4)−O(4)	2.480(6)
Sm(4)−S(12′)	2.763(2)	Sm(4)−S(9)	2.784(3)
Sm(4)−S(7)	2.848(2)	Sm(4)−S(10′)	2.880(3)
Sm(4)−S(11′)	2.909(2)	Sm(4)−S(8)	2.949(2)
S(1)−C(1)	1.771(9)	S(2)−C(7)	1.770(9)
S(3)−C(13)	1.781(9)	S(4)−C(19)	1.753(9)
S(5)−C(25)	1.759(9)	S(6)−C(31)	1.795(9)
S(7)−C(37)	1.790(9)	S(8)−C(43)	1.775(9)
S(9)−C(49)	1.766(9)	S(10)−C(55)	1.770(8)
S(10)−Sm(4″)	2.880(3)	S(11)−C(61)	1.759(9)
S(11)−Sm(4″)	2.909(2)	S(12)−C(67)	1.772(9)
S(12)−Sm(4″)	2.763(2)	Sm(1)−O(1)	2.479(6)
C(1)−S(1)−Sm(2)	121.4(3)	C(1)−S(1)−Sm(1)	114.9(3)
C(7)−S(2)−Sm(1)	104.2(3)	C(7)−S(2)−Sm(2)	118.1(3)
C(13)−S(3)−Sm(2)	125.1(3)	C(13)−S(3)−Sm(1)	113.7(3)
C(19)−S(4)−Sm(3)	115.6(3)	C(19)−S(4)−Sm(2)	125.0(3)
C(25)−S(5)−Sm(3)	117.8(3)	C(25)−S(5)−Sm(2)	115.2(3)
C(31)−S(6)−Sm(2)	119.2(3)	C(31)−S(6)−Sm(3)	110.7(3)
C(37)−S(7)−Sm(3)	119.2(3)	C(37)−S(7)−Sm(4)	120.6(3)
C(43)−S(8)−Sm(3)	104.3(3)	C(43)−S(8)−Sm(4)	123.9(3)
C(49)−S(9)−Sm(4)	118.2(3)	C(49)−S(9)−Sm(3)	116.0(3)
C(55)−S(10)−Sm(1)	111.2(3)	C(55)−S(10)−Sm(4″)	118.7(3)
C(61)−S(11)−Sm(1)	118.6(3)	C(61)−S(11)−Sm(4″)	108.4(3)
C(67)−S(12)−Sm(4″)	105.5(3)	C(67)−S(12)−Sm(1)	118.7(3)

[a] Symmetry transformations used to generate equivalent atoms: (′) $x + 1/2, y - 1/2, z$; (″) $x - 1/2, y + 1/2, z$.

Crystallization of $Sm(SPh)_3$ from THF is also possible and results in a significantly different solid-state structure. From the less basic solvent, light yellow $[(THF)Sm(SPh)_3]_n$ (**4**) was isolated from a hexane-layered solution in 22% yield. Polymer **4** (Figure 3, Table 4) was characterized by low-temperature single-crystal X-ray diffraction and found to contain a 1D array of seven coordinate Sm(III) ions connected through sets of three doubly bridging SPh ligands, with a single THF ligand saturating each Sm(III) coordination sphere. The intense yellow colors of the two Sm thiolates are attributed to a visible S-to-Sm(III) charge-transfer excitation.

Table 5. Significant Bond Lengths (Å) and Angles (deg) for $(THF)_3Er(SePh)_3$[a]

Er(1)−O(1)	2.347(3)	Er(1)−O(1)′	2.347(3)
Er(1)−O(1)″	2.347(3)	Er(1)−Se(1)′	2.7766(7)
Er(1)−Se(1)	2.7766(7)	Er(1)−Se(1)″	2.7765(7)
Se(1)−C(1)	1.930(6)		
O(1)−Er(1)−O(1)′	81.33(12)	O(1)−Er(1)−O(1)″	81.33(12)
O(1)′−Er(1)−O(1)″	81.33(12)	O(1)−Er(1)−Se(1)′	92.35(8)
O(1)′−Er(1)−Se(1)′	172.85(8)	O(1)″−Er(1)−Se(1)′	94.49(8)
O(1)−Er(1)−Se(1)	172.85(8)	O(1)′−Er(1)−Se(1)	94.49(8)
O(1)″−Er(1)−Se(1)	92.35(8)	Se(1)′−Er(1)−Se(1)	91.46(2)
O(1)−Er(1)−Se(1)″	94.49(8)	O(1)′−Er(1)−Se(1)″	92.35(8)
O(1)″−Er(1)−Se(1)″	172.85(8)	Se(1)′−Er(1)−Se(1)″	91.46(2)
Se(1)−Er(1)−Se(1)″	91.46(2)	C(1)−Se(1)−Er(1)	103.28(14)

[a] Symmetry transformations used to generate equivalent atoms: (′) $-y+1, x-y+1, z$; (″) $-x+y, -x+1, z$.

Table 6. Significant Bond Lengths (Å) and Angles (deg) for $[(py)_3Sm(SePh)_3]_2$[a]

Sm−N(2)	2.510(5)	Sm−N(3)	2.579(5)
Sm−N(1)	2.582(5)	Sm−Se(3)	2.8968(11)
Sm−Se(2)	2.9129(14)	Sm−Se(1)	2.9972(11)
Sm−Se(1)′	3.0391(14)	Se(1)−C(1)	1.923(6)
Se(1)−Sm′	3.0391(14)	Se(2)−C(7)	1.910(6)
Se(3)−C(13)	1.912(6)		
N(2)−Sm−N(3)	145.3(2)	N(2)−Sm−N(1)	83.1(2)
N(3)−Sm−N(1)	84.7(2)	N(2)−Sm−Se(3)	79.33(11)
N(3)−Sm−Se(3)	68.32(11)	N(1)−Sm−Se(3)	90.09(11)
N(2)−Sm−Se(2)	102.21(12)	N(3)−Sm−Se(2)	93.93(12)
N(1)−Sm−Se(2)	172.14(10)	Se(3)−Sm−Se(2)	96.58(4)
N(2)−Sm−Se(1)	137.12(11)	N(3)−Sm−Se(1)	74.99(11)
N(1)−Sm−Se(1)	89.82(11)	Se(3)−Sm−Se(1)	143.14(3)
Se(2)−Sm−Se(1)	82.35(4)	N(2)−Sm−Se(1)′	72.66(11)
N(3)−Sm−Se(1)′	137.93(11)	N(1)−Sm−Se(1)′	84.18(11)
Se(3)−Sm−Se(1)′	151.88(2)	Se(2)−Sm−Se(1)′	91.78(4)
Se(1)−Sm−Se(1)′	64.56(3)	C(1)−Se(1)−Sm	115.3(2)
C(1)−Se(1)−Sm′	114.9(2)	Sm−Se(1)−Sm′	115.44(3)
C(7)−Se(2)−Sm	109.4(2)	C(13)−Se(3)−Sm	114.2(2)

[a] Symmetry transformations used to generate equivalent atoms: (′) $-x+1, -y+1, -z-2$.

Ln(SePh)$_3$. Trivalent $Ln(SePh)_3$ coordination complexes can also be prepared by reduction of PhSeSePh with elemental Ln/Hg. The less basic selenolate ligands are more readily displaced by neutral donors from the Ln coordination sphere, and so both THF and pyridine coordination compounds of $Ln(SePh)_3$ are considerably more soluble than their thiolate counterparts. With the later lanthanides, the trivalent benzeneselenolates $(THF)_3Ln(SePh)_3$ (Ln = Tm (**5**), Ho (**6**), Er (**7**)) were isolated, and the structure of **7** was determined by low-temperature single-crystal X-ray diffraction (Figure 4, Table 5); unit cells were obtained to establish that **5**−**7** were isostructural. Complex **7** is a *fac*-octahedral molecule with three crystallographically equivalent Er−X (X = Se, O) bonds. The complex is isostructural with $(THF)_3Yb(SePh)_3$[1i] but is merohedrally twinned.

With the larger Sm ion, oligomeric structures are obtained from both pyridine and THF. From pyridine, red $[(py)_3Sm(SePh)_3]_2$ (**8**) can be isolated in 60% yield, and the structure was determined at low temperature (Figure 5, Table 6). Compound **8** is dimeric in the solid state, with a pair of μ_2-benzeneselenolates connecting the two pentagonal bipyramidal metal centers. The terminal PhSe ligands occupy axial and equatorial positions.

From less basic THF, the earlier lanthanide benzeneselenolates crystallize as coordination polymers in ca. 80% yields. The precise stoichiometry of the Nd complex $[(THF)_4Nd_3(SePh)_9]_n$ (**10**) was established by low-temperature X-ray diffraction (Figure 6, Table 7), and the unit cells of the light green Pr (**9**) and deep red Sm (**11**) analogues indicate these compounds are isostructural to the Nd compound. Polymers **9**−**11** contain a linear 1D array of Ln(III) ions bridged to adjacent metals by a set of three μ_2-SePh ligands, and an alternating number (1-1-2) of THF ligands are coordinated to the array of metal ions in the solid state.

Table 7. Significant Bond Lengths (Å) and Angles (deg) for $[(THF)_4Nd_3(SePh)_9]_n$[a]

Nd(1)−O(1)	2.544(18)	Nd(1)−Se(8)′	2.945(5)
Nd(1)−Se(7)′	2.975(5)	Nd(1)−Se(3)	2.976(5)
Nd(1)−Se(2)	2.976(5)	Nd(1)−Se(9)′	2.989(5)
Nd(1)−Se(1)	3.050(5)	Nd(2)−O(2)	2.407(19)
Nd(2)−Se(3)	2.971(4)	Nd(2)−Se(5)	2.976(5)
Nd(2)−Se(2)	2.987(5)	Nd(2)−Se(6)	2.995(5)
Nd(2)−Se(4)	3.034(5)	Nd(2)−Se(1)	3.072(5)
Nd(3)−O(4)	2.428(17)	Nd(3)−O(3)	2.443(19)
Nd(3)−Se(4)	2.981(5)	Nd(3)−Se(9)	3.032(4)
Nd(3)−Se(7)	3.038(4)	Nd(3)−Se(6)	3.114(4)
Nd(3)−Se(5)	3.131(5)	Nd(3)−Se(8)	3.149(5)
Se(1)−C(1)	1.885(12)	Se(2)−C(7)	1.886(13)
Se(3)−C(13)	1.885(13)	Se(4)−C(19)	1.869(12)
Se(5)−C(25)	1.887(13)	Se(6)−C(31)	1.894(12)
Se(7)−C(37)	1.868(12)	Se(7)−Nd(1)″	2.975(5)
Se(8)−C(43)	1.873(14)	Se(8)−Nd(1)″	2.945(5)
Se(9)−C(49)	1.851(12)	Se(9)−Nd(1)″	2.989(5)
C(1)−Se(1)−Nd(1)	108.1(8)	C(1)−Se(1)−Nd(2)	108.7(7)
C(7)−Se(2)−Nd(1)	114.5(7)	C(7)−Se(2)−Nd(2)	127.9(8)
C(13)−Se(3)−Nd(2)	114.1(7)	C(13)−Se(3)−Nd(1)	117.1(8)
C(19)−Se(4)−Nd(3)	115.8(6)	C(19)−Se(4)−Nd(2)	117.4(7)
C(25)−Se(5)−Nd(2)	111.4(8)	C(25)−Se(5)−Nd(3)	115.2(10)
C(31)−Se(6)−Nd(2)	122.4(8)	C(31)−Se(6)−Nd(3)	120.4(7)
C(37)−Se(7)−Nd(1)″	117.6(7)	C(37)−Se(7)−Nd(3)	117.4(6)
C(43)−Se(8)−Nd(1)″	114.6(9)	C(43)−Se(8)−Nd(3)	124.3(11)
C(49)−Se(9)−Nd(1)″	115.3(8)	C(49)−Se(9)−Nd(3)	115.0(7)

[a] Symmetry transformations used to generate equivalent atoms: (′) $-x+1/2, y-1/2, -z+3/2$; (″) $-x+1/2, y+1/2, -z+3/2$.

The visible electronic excitations of the redox active $Ln(ER)_3$ have been attributed to a chalcogen to metal charge transfer. Here, the assignment is confirmed by resonance Raman experiments on $Sm(SePh)_3$ and $Yb(SePh)_3$ in pyridine solution. Figure 7 shows the Raman spectrum for $Sm(SePh)_3$ in the region between 850 and 950 cm^{-1}. A clear resonance effect is observed as the excitation laser wavelength is tuned from blue (488 nm) to yellow (568 nm). In particular, the intensity of the peak at approximately 900 cm^{-1} increases with respect to the peak at 950 cm^{-1}. The existence of clear resonance enhancement in the Raman spectra is strong experimental evidence for a charge-transfer band.[20] Further evidence for charge transfer is found in the Raman spectra of $Yb(SePh)_3$ (Figure 8). This molecule has a visible absorption band with a maximum at 510 nm, and when it is excited with 514.5 nm light, an even more dramatic resonance effect is observed. Further work is underway to identify these and other Raman active modes.

Discussion

The chemistry of lanthanide chalcogenolate compounds has expanded dramatically in the past few years,[1−6,21] and it is now clear that large, sterically demanding ancillary ligands are not necessary in order to form stable, isolable complexes. An understanding of the relationships between metal ionic radius,

(20) For a discussion of Raman spectroscopy and its applications to inorganic chemistry, see: *Advances in Infrared and Raman Spectroscopy*; Clark, R. J. H., Hester, R. E., Eds.; Wiley Heyden Ltd.: New York, 1975.

(21) Nief, F. *Coord. Chem. Rev.* **1998**, in press.

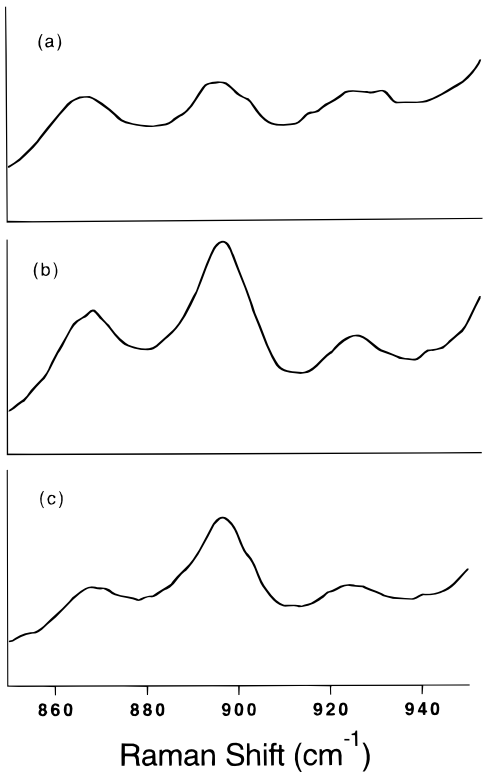

Figure 7. Resonance Raman spectra of $Sm(SePh)_3$ (adsorption λ_{max} = 425 nm) dissolved in pyridine, between 850 and 950 cm^{-1} taken at room temperature. The laser energy decreases from top to bottom. Note the clear enhancement of the mode at 900 cm^{-1}. Key: (a) 488.0 nm (2.54 eV); (b) 514.5 nm (2.41 eV); (c) 568.2 nm (2.18 eV).

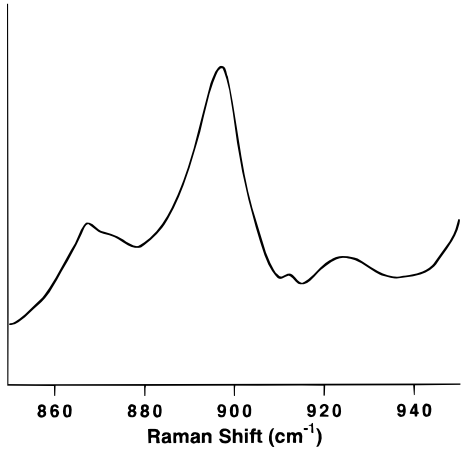

Figure 8. Resonance Raman spectra of $Yb(SePh)_3$ (adsorption λ_{max} = 510 nm) dissolved in pyridine, between 850 and 950 cm^{-1} using a 514.5 nm (2.34 eV) laser excitation at room temperature. Note the clear enhancement of the mode at 900 cm^{-1}.

the E and R of chalcogenolate ligands, and neutral donor ligands and the physical, structural, and chemical properties of $Ln(ER)_x$ complexes is slowly emerging. Trends based on solid-state structure can be assessed, keeping in mind that solid-state and solution structures are not necessarily related.

Both the lanthanide benzenethiolates and selenolates show an increasing tendency to oligomerize as the size of the metal increases. In the benzenethiolate compounds, this trend is best illustrated in the series of pyridine coordination complexes $(py)_3Yb(SPh)_3$,[1g] $[(py)_3Ho(SPh)_3]_2$, and $[(py)_2Sm(SPh)_3]_4$. The benzeneselenolates, when crystallized from weak donor solvents, show a more dramatic change from monometallic octahedral compounds of the smaller metals (Ho, Er, Tm) $(THF)_3Ln(SePh)_3$ to 7,7,8 coordinate $[(THF)_4Ln_3(SePh)_9]_n$ polymers of the early/middle (Pr, Nd, Sm) lanthanides. Diffraction quality crystals of $(THF)_nLn(SePh)_3$ (Ln = Gd−Tb) were not obtained, and solvent loss precluded a definitive analysis of the structure by X-ray powder diffraction. The tendency to bridge larger metals can be attributed to the diminished intercoordination sphere repulsions. These systematic changes in structure with changing metal size contrast significantly with the wide variety of structures found in related metal halide coordination chemistry.[13]

The identity of the chalcogen clearly influences structure. Electrostatically, the smaller, more electronegative SPh ligand should be a stronger donor toward Ln ions than is the larger, less electronegative SePh. The greater tendency of S to bridge metals is reflected in the relative solubility, where, for example, $Ln(SPh)_3$ are sparingly soluble in THF while the selenolates are considerably more soluble. The differing degrees of oligomerization (i.e. $[(py)_3Sm(SePh)_3]_2$ and $[(py)_2Sm(SPh)_3]_4$) can also be rationalized in terms of greater sulfur nucleophilicity, but there are examples (i.e. $(py)_3Yb(SPh)_3$ vs $[(py)_3Tm(SePh)_3]_2$) that indicate chalcogen basicity and chalcogenolate steric effects can have opposing effects.

Chalcogenolate steric properties appear to influence structure not in terms of chalcogen size and repulsion within the primary metal coordination sphere but in terms of secondary coordination sphere interactions. Because of the generally acute Ln−E−C(Ph) angles, an increase of chalcogen size will effectively reduce ligand−ligand repulsion by distancing the benzene substituent, thus permitting either an increase in coordination number or the bridging of the sterically demanding chalcogenolate. This effect has been noted previously in divalent $Ln(EPh)_2$ structures, where, for example, the difference in coordination geometries between octahedral $(py)_4Yb(EPh)_2$ (E = S, Se) and the pentagonal bipyramidal $(py)_5Yb(TePh)_2$ was attributed to the increase in chalcogen size.[1d] A reduction of secondary coordination sphere ligand−ligand repulsion can also account for the different structures of $(py)_3Yb(SPh)_3$ and $[(py)_3Tm(SePh)_3]_2$. In these two molecules, the metal ions have nearly identical ionic radii, and the less nucleophilic selenolates can bridge to form a seven-coordinate structure because the benzene substituents are, on average, 0.14 Å[22] further from the Ln ion. The same rationale can explain the different structures of 7 coordinate Sm(III) ions in polymer **4** and the alternating 7,7,8 coordinate Sm(III) ions in polymer **11**. Again, displacing the Ph group by 0.14 Å (the difference between the ionic radius of S and Se) permits coordination of an additional THF ligand in the Se polymer.

A comparison of $Ln(EPh)_x$ structures with compounds containing bulkier R groups leads to the surprising conclusion that R groups have little impact on $Ln(ER)_x$ coordination chemistry in the solid state. The early description of lanthanide thiolates as insoluble in all common donor solvents[23] clearly inspired the subsequent use of these sterically demanding trisubstituted aryl, alkyl, and $Si(SiR_3)_3$ R groups on the chalcogen in order to decrease the tendency of chalcogen to bridge Ln ions. Somewhat surprisingly, the coordination chemistry of these sterically hindered $Ln(ER)_x$ and the corresponding $Ln(EPh)_x$ are similar. For example, both the 2,4,6-tri-*tert*-butylbenzyl and benzyl thiolates form 6 coordinate pyridine complexes with Yb(III) and the benzenethiolate forms seven coordinate Sm(III) complexes in either THF or pyridine,[2d,e] while the tri-*tert*-butylbenzenethiolate yields an octahedral

(22) Shannon, R. D. *Acta Crystallogr.* **1976**, *A32*, 751.
(23) Gharia, K. S.; Singh, M.; Mathur, S.; Roy, R.; Sankhla, B. S. *Synth. React. Inorg. Met.-Org. Chem.* **1982**, *12*, 337.

compound. Even the $E-Si(SiR_3)_3$ ligands appear to have only a moderate effect on structure; i.e., compare the seven coordinate selenolates of La and Ce with the 7,7,8 coordinate polymer **11** or the 7 coordinate Eu(II) complexes (i.e. the phosphine coordination complex of $Eu(SeSi(SiMe_3)_3)_2$[3b] with the seven coordinate $Eu(SePh)_2(THF)_3$ or octahedral $(py)_2Eu(SePh)_2$ coordination polymers.[1b] This lack of impact on structure can be attributed to the flexibility of the bond angle at the chalcogen. With terminal Ln−E−Ph angles ranging from 98 to 120°, the steric demands of the benzene substituent are already considerable. Sterically "more demanding" ligands are accommodated by simply opening the Ln−E−C angles, i.e., 116−126° in the $(THF)_3Sm(SR)_2$ dimer, 122−7° in $THF_3Sm(SR)_3$,[2d] or, even more dramatically, 163−4° in $Ln(ESi(SiR_3)_3)_2$.[3b]

As expected, stronger bases[24] displace bridging chalcogenolates from Ln(III) ions more efficiently. Macroscopically, this effect is evident in the greater solubility of $Ln(SPh)_3$ in pyridine relative to THF. On a molecular level, donor base strength is evident in the structures of $[(THF)_4Sm_3(SePh)_9]_n$ and $[(py)_3Sm(SePh)_3]_2$. In the weaker THF donor, $Sm(SePh)_3$ crystallizes as a one-dimensional polymer with six bridging selenolates per 7,7,8 coordinate Sm(III) ion, whereas the stronger pyridine donor disrupts bridging interactions more efficiently and a structure with only two bridging benzeneselenolates per 7 coordinate metal is observed.

The intense colors of the redox active $Ln(ER)_3$ complexes have been attributed, on a tentative basis, to a charge-transfer excitation from the chalcogenolate ligand to the Ln ion. Given the same metal (i.e. $Yb(SPh)_3$ vs $Yb(SePh)_3$), the energy of this absorption decreases as the chalcogen electronegativity decreases,[1h] given the same chalcogen (i.e. red $Eu(SPy)_4^-$ vs colorless $Tm(SPy)_4^-$),[5a] the energy of the absorption decreases as the stability of the Ln(II) ion increases, and given the same metal and ligand, a smaller but still distinct change in energy is noted when the solvent changes (compound **8**, $\lambda_{max} = 425$ nm, vs compound **11**, $\lambda_{max} = 409$ nm). A LMCT assignment would also explain the color of three coordinate $Sm(SR)_3$, which is described as deep orange.[5a] This charge transfer excitation is shifted considerably into the visible spectrum, relative to the yellow SPh compounds **3** and **4**, because the three coordinate Sm(III) ion is relatively electron poor and the alkyl substituent localizes electron density on the S, thus rendering the electron transfer from S to Sm relatively facile. The resonance Raman experiments here show typical resonance enhancement, thus confirming the LMCT assignment.

The majority of $Ln(ER)_x$ decompositions have to date yielded the anticipated solid-state product: $Ln(ER)_2$ gives LnE and $Ln(ER)_3$ gives Ln_2E_3. The deviations from this behavior were noted only in the thermolysis of the trivalent europium thiolate $Eu(SPy)_4^-$, which decomposes to give EuS,[4a] and the holmium benzeneselenolate $Ho(SePh)_3$, which gave a mixture of HoSe/$HoSe_2$.[1g] While the Eu thermolysis is understandable in terms of the relative instability of Eu_2S_3, the latter example was curious and suggests that solution thermolysis of these molecules could potentially lead to the formation of LnE nanoclusters. To determine whether this reactivity could be extended to sulfido compounds, **1** and **2** were decomposed thermally, and the solid-state products were examined by X-ray powder diffraction. When the thermolysis temperature was kept below 400 °C in an attempt to isolate metastable LnS/LnS_2 phase mixtures, no crystalline product was observed in the X-ray powder diffraction profile. Only at elevated temperatures (>550 °C) did the thermolysis of **1** or **2** give a crystalline solid-state product that was identified, by XRPD, as the thermodynamically stable Ln_2S_3 phase.

Acknowledgment. This work was supported by the National Science Foundation, under Grant CHE-9628834. F.H.L. thanks the Rutgers Research Council for support.

Supporting Information Available: Six X-ray crystallographic files, in CIF format, are available. Access information is given on any current masthead page.

IC9716161

(24) (a) Schlesener, C. J.; Ellis, A. B. *Organometallics* **1983**, *2*, 529. (b) Brennan, J. G.; Stults, S.; Andersen, R. A.; Zalkin, A. *Inorg. Chim. Acta* **1987,** *139*, 201. (c) Brennan, J. G.; Stults, S.; Andersen, R. A.; Zalkin, A. *Organometallics* **1988**, *7*, 1329.